



저작자표시-비영리-변경금지 2.0 대한민국

이용자는 아래의 조건을 따르는 경우에 한하여 자유롭게

- 이 저작물을 복제, 배포, 전송, 전시, 공연 및 방송할 수 있습니다.

다음과 같은 조건을 따라야 합니다:



저작자표시. 귀하는 원저작자를 표시하여야 합니다.



비영리. 귀하는 이 저작물을 영리 목적으로 이용할 수 없습니다.



변경금지. 귀하는 이 저작물을 개작, 변형 또는 가공할 수 없습니다.

- 귀하는, 이 저작물의 재이용이나 배포의 경우, 이 저작물에 적용된 이용허락조건을 명확하게 나타내어야 합니다.
- 저작권자로부터 별도의 허가를 받으면 이러한 조건들은 적용되지 않습니다.

저작권법에 따른 이용자의 권리는 위의 내용에 의하여 영향을 받지 않습니다.

이것은 [이용허락규약\(Legal Code\)](#)을 이해하기 쉽게 요약한 것입니다.

[Disclaimer](#)

보건학석사 학위논문

Source Apportionment and
Oxidative Potential of
Organic Compounds in PM₁
in Seoul, Korea

서울시 PM₁ 유기화학성분의
오염원 추정과 산화 잠재력 평가

2022년 8월

서울대학교 대학원

환경보건학과 환경보건학전공

류 지 원

Source Apportionment and Oxidative Potential of Organic Compounds in PM₁ in Seoul, Korea

지도교수 이승묵

이 논문을 보건학석사 학위논문으로 제출함
2022년 5월

서울대학교 대학원
환경보건학과 환경보건학전공
류 지 원

류지원의 보건학석사 학위논문을 인준함
2022년 7월

위 원 장 _____ 김화진 (인)

부위원장 _____ 이지이 (인)

위 원 _____ 이승묵 (인)

Abstract

Source Apportionment and Oxidative Potential of Organic compounds in PM₁ in Seoul, Korea

Jiwon Ryu

Department of Environmental Health Science

The Graduate School of Public Health

Seoul National University

Seoul, Korea is an urbanized megacity with commercial, industrial, and residential areas and is affected by transporting air pollutants from China and Japan, the atmospheric chemical composition is very complicated. Especially in urban or industrial areas, organic carbon (OC) and elemental carbon (EC) have a high composition ratio. Therefore, identifying the chemical properties and source contribution of organic compounds and estimating their health effects must be performed to establish appropriate reduction policies. This study is the first to estimate the source contribution of organic pollutants and evaluate their oxidative potential in Seoul.

A total of 91 PM₁ samples were collected over seven months (September 2021 to March 2022) in Seoul, Korea. These samples

were analyzed for PM₁ mass concentration, organic carbon (OC), elemental carbon (EC), and 56 organic compounds. As a results of the Positive Matrix Factorization (PMF) receptor model for identifying source contribution, five source categories were identified: Mobile (24%), SOA + Biomass burning (39%), Anthropogenic SOA (6.2%), Biogenic SOA (15%), and Combustion related (17%). In addition, the cluster analysis, the Conditional Bivariate Probability Function (CBPF) model, and the Potential Source Contribution Function (PSCF) model were performed to estimate the regional and long-range transporting impacts of each source.

As a result of estimating the OP through dithiothreitol (DTT) assay, SOA + Biomass burning source influenced from long distance regions such as Mongolia, North China, and North Korea was major contributor to OP. Also, PAHs, sugars, glyserides, methoxyphenols, and resin acids released dominantly from biomass burning, coal and wood combustion were high correlated with OP. Therefore, SOA + Biomass burning source, which contributes the most to OC in Seoul and has a high correlation with OP, must be managed.

Keyword: PM₁, Organic compounds, Source apportionment, Oxidative potential

Student Number: 2020–20616

Table of Contents

1. Introduction	1
2. Data and Method.....	3
2.1 Sampling.....	3
2.2 Analytical procedure.....	3
2.3 Receptor model.....	5
2.3.1 The positive matrix factorization (PMF) model.....	5
2.3.2 The cluster analysis.....	6
2.3.3 The potential source contribution function (PSCF) model....	7
2.3.4 The conditional bivariate probability function (CBPF) model.....	7
2.4 The dithiothreitol(DTT) assay.....	8
3. Results and discussions.....	9
3.1 Chemical components of PM ₁	9
3.2 Source apportionment.....	15
3.3 DTT activity results.....	23
4. Conclusion	25
References.....	28
Supplementary Materials.....	33
국문 초록	37

List of Tables

Table 1. Uncertainty calculation method for each species.....	6
Table 2. Quantification results ($\mu\text{g}/\text{m}^3$) for OC and EC	10
Table 3. Analyzed non-polar organic compounds	11
Table 4. Analyzed polar organic compounds.....	12
Table 5. Quantification results (ng/m^3) for organic compounds	13
Table 6. Average source contribution of each factor.....	20
Table 7. Multiple linear regression (MLR) analysis between OP _{dt} and source contributions	25
Table 8. Pearson correlations between the OP _{dt} and the chemical species	25

List of Figures

Figure 1. Average concentration of total organic compounds	14
Figure 2. (a) Diagnostic ratios for the sources of PAHs, (b) Scatter plots of pyrene versus fluoranthene	14
Figure 3. Source profiles of PM ₁ OC	17
Figure 4. Time series of source contribution.....	18
Figure 5. The Result of cluster analysis	19
Figure 6. The fraction (%) of source contribution for each factor	20
Figure 7. The CBPF results for (a) OC, (b) Mobile, (c) Anthropogenic SOA, (d) Biogenic SOA, (e) Combustion related, (f) SOA + Biomass burning	21
Figure 8. The PSCF results ofr (a) SOA + Biomass burning, (b) Combustion related, (c) Anthropogenic SOA, (d) Biogenic SOA	23
Figure 9. Scatter plot and temporal variation of DTT consumption rate (nmol/min/m ³) with OC concentration (μg/m ³).....	24

1. Introduction

Airborne particulates, particulate matter (PM) is chemically and physically non-specific and emitted from various natural and anthropogenic sources or produced secondary by chemical reactions (Russell and Allen, 2004). In particular, PM_{2.5} (PM with aerodynamic diameter $< 2.5 \mu\text{m}$) has been the focus of several studies due to its physicochemical characteristics, diverse sources, and harmful health effects (Breton et al., 2012, Ni et al., 2015, Pope III et al., 2011). Epidemiological and toxicological research have suggested that particulate matter (PM) cause adverse health effects, especially the PM₁ can penetrate deep into the alveolar region of the lungs, pass through lung tissue, penetrate biological membranes, and circulate in the bloodstream (Cai et al., 2022). Exposure to PM₁ is associated with augmented risks of cardiovascular mortality and respiratory morbidity and mortality (Liu et al., 2013, Lin et al., 2016, Cheng et al., 2011, Mei et al., 2022). However, relatively few studies on PM₁ have been conducted, and no national air quality standards have been prepared. Therefore, research and data accumulation on PM₁ are essential.

Seoul, Korea is the urbanized megacity with high population density, also it is surrounded by China and Japan. Since Seoul is influenced by transport of air pollutants from these areas in addition to various regional sources, atmospheric chemical composition is very complicated, especially in urban or industrial areas, organic carbon(OC) and elemental carbon (EC) has a high composition ratio.

Therefore, by monitoring the chemical characteristics of PM₁ organic components collected in Seoul, the PMF model was used to identify source apportionment and the contribution of each source contributions. In addition, the cluster analysis, the Conditional

Bivariate Probability Function (CBPF) model, and the Potential Source Contribution Function (PSCF) model were performed to estimate the regional and long-range transporting impacts of each source.

Oxidative potential (OP) has been proposed as a useful descriptor for the ability of particulate matter to produce reactive oxygen species (ROS) (Lin and Yu, 2019). Methods for estimating the oxidative potential are classified into cellular assays and cell-free assays. The dithiothreitol (DTT) assay is the most frequently used method of the cell-free assay (Liu et al., 2018, Jiang et al., 2019). Therefore, through this method, it is possible to indirectly estimate the health effects according to the difference in the chemical composition of PM₁. According to existing studies, the oxidative potential and organic compounds has high correlation (Yang et al., 2014, Biswas et al., 2009, Cho et al., 2005, Verma et al., 2014). It indicates the importance of organic compounds on the ROS generation potential in the body (Fang et al., 2015). In addition, it is possible to statistically estimate highly correlated sources with OP through the multiple linear regression analysis.

The objectives of this study are 1) to provide as a reference to chemical characteristics and source apportionment of organic compounds in PM₁ in Seoul 2) to predict oxidative potential of PM₁ in Seoul by relating chemical constituents and sources to ROS activity 3) to provide scientific evidence for policy makers to prioritize sources to be regulated.

2. Data and Method

2.1. Sampling

A total of 91 samples were collected every second days for 23h from September 2021 to March 2022 on the roof of the Graduate School of Public Health building at Seoul National University, Seoul, Korea (32.465° N, 126.954° E; 27m above ground level). The sampling site is located in the mixed commercial, residential, and high traffic area.

Samples for PM₁ mass concentration, organic carbon(OC), and elemental carbon(EC) analyses were collected using low-volume air sampler with filter pack (URG-2000-30FG, URG, USA) and cyclone (URG-2000-30EH, URG, USA) at the flow rate of 16.7 L/min. Teflon filters (PT48P-KR, MTL, USA) were used to measure mass concentration by weighing the filters using a microgram balance (sensitivity ± 0.01 mg; CPA225D/Quintix125D, Sartorius, Germany). Prior to sampling, Quartz fiber filters (TISSUE QUARTZ 2500 QUT-UP 7202, PALL science, USA) used to measure OC and EC concentration were pre-baked 450°C for 12h to remove organic contaminants.

Samples for organic compounds analysis were collected using a high-volume air sampler (TE-HVPLUS, TISCH, USA) at the flow rate of 40 CFM with Quartz microfiber filters (20.3 x 25.4 cm²) and impactor filter (TE-230-QZ, TISCH, USA). It was also pretreated in the same way.

2.2. Analytical procedure

To analyze OC and EC concentrations, carbon aerosol analyzer

(Sunset Laboratory Inc., USA), using thermal optical transmittance (TOT) method, and the National Institute for Occupational Safety and Health (NIOSH) 870 protocol was used for the data quantification.

To analyze organic compounds, Gas chromatography/mass spectrometer (7890B/5977B, Agilent, USA) was used. The filters punched in size 4cm x 24cm were extracted in Dichloromethane: Methanol (3:1, v/v) using sonicator at 0°C for 1hr. After extraction, samples were concentrated using N₂ gas in Turbovap II (Zymark Co., USA) and filtered using syringe filter (Acrodisc Syringe filters with PTFE membrane, PALL science). After filtering, the samples were finally concentrated to 1ml using a Reacti-Therm (Thermo-Science, TS18822, USA) and stored it in freezer until analysis.

In addition, to silylate polar organic compounds, 50 μ l N,O-bis – (trimethylsilyl) trifluoroacetamide (BSTFA) with 1% trimethylchlorosilane (TMCS) (99%, Sigma Aldrich, USA) and 50 μ l of pyridine (HPLC grade, Sigma Aldrich, USA) were added to 50 μ l of final concentrated samples and reacted at 75°C for 90 min.

A total of 67 non polar and 51 polar compounds were quantified using 6 points of calibration standards with 12 types of internal standards (eicosane-d42, tetracosane-d50, triacontane-d58, doriacontane-d66, hexatriacontane-d74, benzo[a]anthracene-d12, coronene-d12, chloestane-d4, decanoic acid-d19, tetracosanoic acid-d59, succinic acid-d4, levoglucosan-C13) for the calculation of the recovery.

The quality assurance and quality control (QA/QC) of organic compounds analyses was performed. First, the calibration curves using 6 levels of native standards is updated at each analysis to check the GC/MS status, and coefficient of determination (r²) was 0.98 or higher. Second, the method detection limits (MDLs) were calculated

using the EPA-specified MDLs calculation method, and concentrations lower than these values were treated as ‘Not detected (N.D)’ values. The MDLs were calculated by multiplying the standard deviation of the lowest concentration of the standard 7 times by the t-value (3.707) of the 99% confidence single tailed. Third, the recovery was calculated by internal & surrogate standard recovery method. The amount lost in the pretreatment process was corrected by checking the concentration recovered by injecting the surrogate standard into each sample.

2.3. Receptor model: positive matrix factorization

2.3.1. The positive matrix factorization (PMF) model

Receptor modeling is based on the idea that mass conservation can be assumed and a mass balance analysis can be used to identify and apportion sources of airborne PM in the atmosphere (Hopke, 1991). The Positive Matrix Factorization (PMF) model is a multivariate receptor model which estimated the source profiles and source contribution based on a least-squares approach (Paatero, 1997). The notation of the PMF is

$$x_{ij} = \sum_{k=1}^p g_{ik} \cdot f_{kj} + e_{ij}$$

Where x_{ij} is the j_{th} species concentration measured in the i_{th} samples and g_{ik} is the airborne mass concentration ($\mu g/m^3$) from the k_{th} source contributing to the i_{th} sample, f_{kj} is the j_{th} species fraction ($\mu g/\mu g$) from the k_{th} source contributing to the i_{th} sample, f_{kj} is the j_{th} species fraction ($\mu g/\mu g$) from the k_{th} source, e_{ij} is the residual associated with j_{th} species concentration measured in the i_{th} sample, and p is the total number of independent sources. PMF provides a

solution that minimizes an object function, $Q(E)$, based upon the uncertainties of each observation (Polissar et al., 1998). This function is defined as

$$Q(E) = \sum_{i=1}^n \sum_{j=1}^m \left[\frac{x_{ij} - \sum_{k=1}^p g_{ik} f_{kj}}{u_{ij}} \right]^2$$

Where u_{ij} is an uncertainty estimate for the j -th constituent measured in the i -th sample. In this study, source identification and apportionment were performed based on the EPA PMF model (EPA PMF5.0). Allocating uncertainty appropriately to the observed data is an important part because the application of the PMF model depends mainly on estimated uncertainties (Heo et al., 2013). The method of calculating the uncertainty of each species is shown in [Table 1]

Table 1. Uncertainty calculation method for each species

Species	Uncertainty equation
Organic carbon	$\sqrt{((0.05 + E^*) \cdot \text{conc.} + 0.1)^2 + (\text{sd. of blank conc.})^2}$
Organic compounds	$\sqrt{(0.15 \cdot \text{conc.})^2 + (0.5 \cdot \text{MDLs})^2}$

*E: Sampling error: (Flow rate/16.7 LPM) X 16.7 LPM

2.3.2. The cluster analysis

The trajectories generated using the HYSPLIT model were separated into groups with similar velocities and directions through cluster analysis, and a general air trajectory inflow pattern was confirmed. Global Data Assimilation System data (GDAS 1.0) with a resolution of $1.0^\circ \times 1.0^\circ$ was used, and the starting height was half of the mixing height, and 96 hours of backward trajectory was used.

2.3.3. The potential source contribution function (PSCF) model

To identify the likely source locations for long-range transboundary aerosols, the potential source contribution function (PSCF) model was performed using PMF resolved-source contribution and 96hr back trajectory. This function is defined as

$$\text{PSCF} = \frac{m_{ij}}{n_{ij}}$$

Where n_{ij} is the total number of end points that fall in the ij th cell, and m_{ij} is the number of end points in the same cell associated with samples that exceed the threshold criterion. In this study, the upper 25th percentile contribution of each source was used as the threshold criterion. To reduce the effect of small values of n_{ij} , weighting function W_{ij} was used. The weighing is calculated as

$$w = \begin{cases} 1.0, (n > 3n_{avg}) \\ 0.8, (2n_{avg} < n < 3n_{avg}) \\ 0.6, (n_{avg} < n < 2n_{avg}) \\ 0.4, (0.5n_{avg} < n < n_{avg}) \\ 0.2, (n < 0.5n_{avg}) \end{cases}$$

2.3.4. The conditional bivariate probability function (CBPF)

To access the likely location of local point sources, a conditional bivariate probability function (CBPF) was used to estimate the factor contribution by PMF analysis coupled with the time-resolved wind directions and speed. CBPF estimated the probability which will exceed a predetermined threshold criterion at a given source contribution from a given wind direction. This function is defined as

$$\text{CBPF} = \frac{m_{\theta j}}{n_{\theta j}}$$

Where $m_{\theta j}$ is the number of samples in the wind sector θ and wind speed interval j greater than the threshold criterion and $n_{\theta j}$ is the number of samples in the same wind direction-speed interval. In this

study, the upper 25th percentile contribution of each source was used as the threshold criterion. Wind direction and speed were observed by the Korea Meteorological Administration's Automated Synoptic Observing System.

2.4. The dithiothreitol (DTT) assay

The oxidative potential (OP), representing the capacity of particulate matter to oxidize molecules with generation of reactive oxygen species (ROS), is useful descriptor of PM toxicity (Fang et al., 2015). The dithiothreitol (DTT) assay uses a chemical redox reaction to determine the amount of ROS produced, and it is most frequently used acellular method to evaluate the OP of PM (Cho et al., 2005, Charrier and Anastasio, 2012). Compared to the cellular assays, DTT assay has the advantage of faster reading speed, lower price, less control environments.

PM samples were extracted via sonication in 100% methanol. The extraction solution 3.5ml was mixed with 0.5mM potassium phosphate buffer (PBS) 1ml, 1mM DTT 0.5ml and incubated at 37°C for 5,10,15,25, and 30 min. The 100 μ l aliquot of the incubated mixture was mixed with 1% TCA(Tri) 1ml, 0.08M Tris buffer 2ml, 0.2mL DTNB (5,5-dithio-bis-2-nitrobenzoic acid) 0.5ml. Reaction between the residual DTT and DTNB forms a light absorbing product, 2-nitro-5-thiobenzoic acid (TNB), which has extinction coefficient of $14150\text{M}^{-1}\text{cm}^{-1}$ at 412 nm wavelength. Then, measure the absorbance using a UV/vis spectrometer. A decreasing absorption intensity for a samples reflects the DTT oxidation over time. The OP is defined by the rate of DTT consumption, and it was determined from the slope and intercept of linear regression of measured absorbance versus time as shown as

$$\sigma DTT = -\sigma Abs \cdot \frac{N_0}{Abs_0}$$

$$DTT_{activity} = \frac{\sigma DTT_{sample} - \sigma DTT_{blank}}{V_{air}}$$

where σAbs (Abs/min) is the slope of absorbance versus time, Abs_0 is the initial absorbance calculated from the intercept of the linear regression of absorbance versus time, N_0 (nmol) is the initial moles of DTT added in the reaction vial. The final DTT activity for a sample was calculated by subtracting a blank value from sample and normalized by sample air volume.

3. Results and discussions

3.1. Chemical components of PM₁

The average PM₁ mass concentration for entire sampling period is $18 \pm 16 \mu g/m^3$. The average OC and EC concentration for entire sampling period is $4.2 \pm 1.9 \mu g/m^3$, $0.30 \pm 0.13 \mu g/m^3$, respectively. The monthly average concentrations are presented in [Table 2]. The OC and EC concentration in January was the highest at $5.7 \pm 1.9 \mu g/m^3$, $0.41 \pm 0.15 \mu g/m^3$, respectively. The average concentrations for entire sampling period of PAHs was $2.8 \pm 1.9 ng/m^3$, n-Alkanes was $13 \pm 24 ng/m^3$, Hopanes & Steranes was $0.03 \pm 0.04 ng/m^3$, Aliphatic diacids was $9.5 \pm 8.5 ng/m^3$, Bezenecarboxylic acids was $4.0 \pm 2.2 ng/m^3$, Alkanoic acids was $7.2 \pm 8.5 ng/m^3$, Sugar & Glyserides was $27 \pm 9.5 ng/m^3$, Fatty acids was $11 \pm 3.2 ng/m^3$, Sterols was $3.9 \pm 0.06 ng/m^3$, Methoxyphenols was $2.9 \pm 0.40 ng/m^3$, Resin acids was $2.6 \pm 1.6 ng/m^3$. The monthly average concentrations are presented in [Table 5], and the overall trend of organic compounds was shown in [Figure 1].

The diagnostic ratio method for PAHs have been applied to identify the possible sources (Tsapakakis and Stephanou, 2005, Hong et al., 2007, Vasilakos et al., 2007, Kong et al., 2010). For the ratio of Flt/(Flt+Pyr), lower than 0.4 is identified petroleum source, and as petroleum combustion if it ranged from 0.40 to 0.50, and biomass and coal combustion sources if it exceeds 0.5 (Xingru et al., 2009). For the ratio of Anthr/(Anthr+Phen) lower than 0.1 is taken as indication of petroleum, while ratio exceeding 0.1 indicates a dominance of combustion source (Han et al., 2011). In this study, the ratio of Flt/(Flt+Pyr) is ranged from 0.57 to 1, and Anthr/(Anthr+Phen) is ranged from 0.54 to 0.73. The results indicated that the PAHs were mainly derived from biomass burning and combustion related sources.

In addition, through the slope of PAHs, the characteristics of sources can be identified (Gao et al., 2011). For the slope of Pyr/Flt, 1.42 indicates vehicle source (He et al., 2008), 0.96 indicates biomass burning (Sheesley et al., 2003), 0.6~0.9 indicates industrial coal combustion (Zhang et al., 2008b). In this study, the slope of Pyr/Flt was 0.7168, and this result suggesting the dominance of biomass burning and coal combustion related sources.

Table 2. Quantification results ($\mu\text{g}/\text{m}^3$) for OC and EC

Monthly average ($\mu\text{g}/\text{m}^3$) \pm stdev.	Sep	Oct	Nov	Dec	Jan	Feb	Mar
Organic Carbon	2.5 ± 1.5	3.0 ± 1.1	4.0 ± 1.9	4.6 ± 1.7	5.7 ± 1.9	4.5 ± 1.6	3.9 ± 1.4
Elemental Carbon	0.21 ± 0.08	0.26 ± 0.07	0.26 ± 0.10	0.37 ± 0.14	0.41 ± 0.15	0.31 ± 0.10	0.24 ± 0.09

Table 3. Analyzed non-polar organic compounds

PAHs (13)	n-Alkanes (8)
2,6-Dimethylnaphthalene	n-C20
Phenanthrene	n-C21
Anthracene	n-C22
9-Methylantracene	n-C23
Fluoranthene	n-C24
Pyrene	n-C25
Benzo [ghi] fluoranthene	n-C26
Benzo [a] anthracene	n-C27
Chrysene	
Benzo [b] fluoranthene	Hopanes & Steranes (3)
Benzo [k] fluoranthene	ABB-20R-C27-Cholestane
Indeno[1,2,3-cd]pyrene	ABB-20R-C28-Methylcholestane
Benzo [ghi] perylene	17A (H) -22,29,30-Trisnorhopane

Table 4. Analyzed polar organic compounds

Aliphatic diacids (10)	Sugar & Glyserides (4)
Malonic (C3)	Mannosan
Maleic (C3=)	Levogluconan
Succinic (C4)	Monopalmitin (16:0)
Fumaric (C4=)	Monostearin (18:0)
Glutaric (C5)	Fatty acids (4)
Adipic (C6)	Pinonic acid
Pimelic (C7)	Linoleic acid
Suberic (C8)	Octacosanoic acid
Azelaic (C9)	Tricontanoic acid
Sebacic (C10)	
Bezenecarboxylic acids (10)	Sterol (1)
Phthalic acid (1,2)	Stigmastanol
Terephthalic acid (1,4)	Methoxyphenols (2)
Methylphthalic acids	4-Hydroxy-3-methoxycinnamaldehyde
Alkanoic acids (5)	3,5-Dimethoxy-4-hydroxycinnamaldehyde
C16:0	Resin acids (3)
C18:0	Iso-Pimaric acid
C20:0	Abietic acid
C22:0	Dehydroabietic acid
C24:0	

Table 5. Quantification results (ng/m³) for organic compounds

Monthly average (ng/m ³) ± stdev.	Sep	Oct	Nov	Dec	Jan	Feb	Mar
PAHs	1.0 ±0.07	1.4 ±0.41	1.8 ±0.40	3.7 ±1.9	5.3 ±2.3	3.4 ±0.96	1.9 ±0.82
n-Alkanes	1.7 ±0.19	18 ±24	5.4 ±15	14 ±27	23 ±32	15 ±21	9.7 ±22
Hopanes & Steranes	0.00 ±0.01	0.03 ±0.04	0.00 ±0.00	0.00 ±0.01	0.06 ±0.05	0.06 ±0.04	0.00 ±0.00
Aliphatic diacids	4.8 ±2.0	20 ±13	9.5 ±7.1	10 ±7.7	8.3 ±5.0	5.7 ±2.1	5.4 ±1.5
Bezene -carboxylic acids	2.6 ±1.2	2.3 ±1.5	5.2 ±2.5	4.1 ±1.9	4.5 ±2.2	4.9 ±2.6	3.2 ±1.0
Alkanoic acids	1.8 ±0.50	3.8 ±3.5	4.2 ±3.1	10 ±15	9.8 ±8.0	5.3 ±3.8	13 ±8.0
Fatty acids	10 ±4.6	13 ±3.2	13 ±5.0	11 ±1.1	11 ±1.1	11 ±1.9	11 ±2.7
Sugar & Glyserides	17 ±9.0	26 ±12	24 ±9.3	32 ±6.5	35 ±5.2	28 ±6.0	24 ±6.3
Sterols	3.9 ±0.01	3.9 ±0.11	3.9 ±0.02	3.9 ±0.04	3.9 ±0.03	3.9 ±0.02	3.9 ±0.08
Methoxy -phenols	2.5 ±0.57	2.8 ±0.40	3.0 ±0.27	3.2 ±0.34	3.1 ±0.29	2.8 ±0.10	2.8 ±0.49
Resin acids	1.3 ±0.56	1.5 ±0.49	2.0 ±0.67	4.0 ±2.7	3.9 ±1.5	2.5 ±0.55	1.8 ±0.59

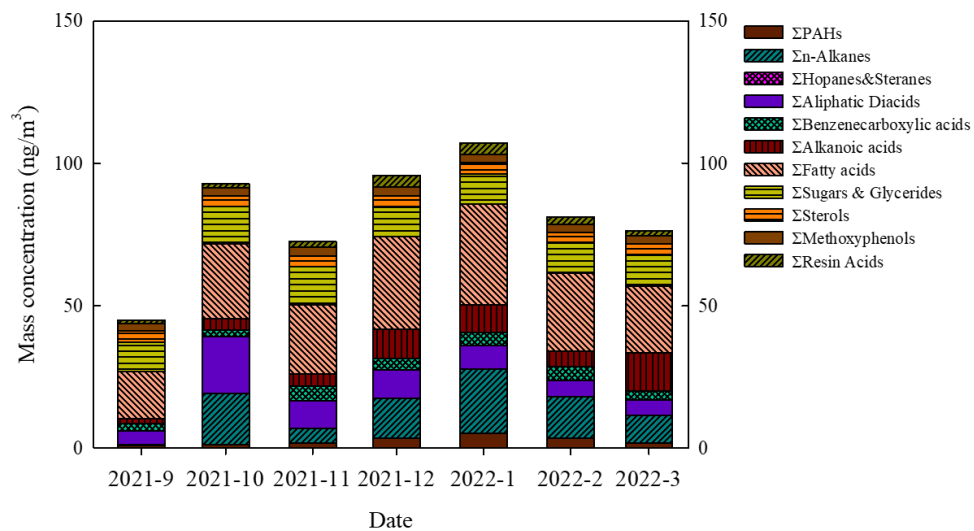


Figure 1. Average concentration of total organic compounds

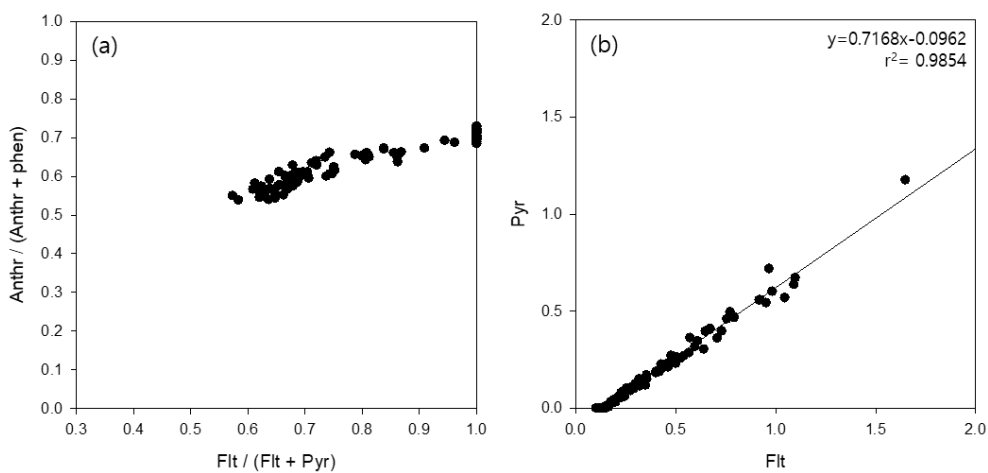


Figure 2. (a) Diagnostic ratios for the sources of PAHs, (b) Scatter plots of Pyrene versus Fluoranthene.

3.2. Source apportionment

3.2.1. PMF results

The compounds used in PMF are OC, EC, PAHs (13), n-Alkanes (8), Hopanes & Steranes (3), Aliphatic diacids (10), Benzenecarboxylic acids (3), Sugar & Glycerides (2), Fatty acids (4), Sterols (1), Methoxyphenols (2), Resin acids (3).

As a results of PMF model, five sources were identified as contributing sources to ambient OC: Mobile (24%), SOA + Biomass burning (39%), Anthropogenic SOA (6.2%), Biogenic SOA (15%), Combustion related (17%).

1) Factor 1: Mobile

The contributions of mobile factor accounted for 24% to OC and average contribution is $0.88 \mu\text{g}/\text{m}^3$. This factor was characterized by high contributions of n-C_{23~27}, 2,6-Dimethylnaphthalene, 9-Methylnaphthalene, ABB-20R-C₂₇-Cholestane, ABB-20R-C₂₈-Methylcholestane, 17A(H)-22,29,30-Trisnorhopane. As EC and hopanes are used as markers for diesel vehicles (Schauer et al., 1999) and steranes are used as markers for gasoline vehicles (Schauer et al., 2002, Wu et al., 2018), the mobile factor in Seoul comprises of both gasoline and diesel vehicle exhaust.

2) Factor 2: SOA + Biomass burning

The contributions of SOA + Biomass burning factor accounted for 39% to OC and average contribution is $1.5 \mu\text{g}/\text{m}^3$. This factor was characterized by high contributions of phthalic acids and mannosan. Phthalic acid and terephthalic acid are marker for anthropogenic SOA, and these are produced from photochemical oxidation of PAHs

(Sheesley et al., 2004, Baltensperger et al., 2005). Mannosan is marker for wood combustion. Therefore, this factor is mixed with SOA and biomass burning sources. In addition, it showed a high contribution between December to February. This tendency seems to reflect the characteristics of biomass burning well.

3) Factor 3: Anthropogenic SOA

The contributions of anthropogenic SOA factor accounted for 6.2% to OC and average contribution is $0.23 \mu\text{g}/\text{m}^3$. This factor was characterized by high contributions of malonic, maleic, succinic, glutaric, adipic, pimelic, suberic, azelaic, and sebacic. Aliphatic dicarboxylic acids are known indicators of anthropogenic SOA which are formed through photochemical oxidation process of pollutants (Shrivastava et al., 2007, Choi et al., 2012).

4) Factor 4: Biogenic SOA

The contribution of biogenic SOA factor accounted for 15% to OC and average contribution is $0.56 \mu\text{g}/\text{m}^3$. This factor was characterized by high contributions of pinonic acid, which is a marker for biogenic SOA, and the major products of photochemical oxidation of monoterpenes derived from biogenic origins (Zhang et al., 2010).

5) Factor 5: Combustion related

The contributions of Biomass burning factor accounted for 17% to OC and average contribution is $0.64 \mu\text{g}/\text{m}^3$. This factor was characterized by high contributions of phenanthrene, fluoranthene, pyrene, indeno[1,2,3-cd]pyrene, chrysene, benzo[b]fluoranthene, benzo[k]fluoranthene, benzo[ghi]fluoranthene, benzo[a]anthracene, n-C_{20~22}, dehydroabietic acid. These PAHs are known indicators

of coal combustion source (Zhang et al., 2008a). Dehydroabietic acid are marker for wood combustion. In addition, this factor showed a high contribution between December to February. This tendency seems to reflect the characteristics of combustion related sources well.

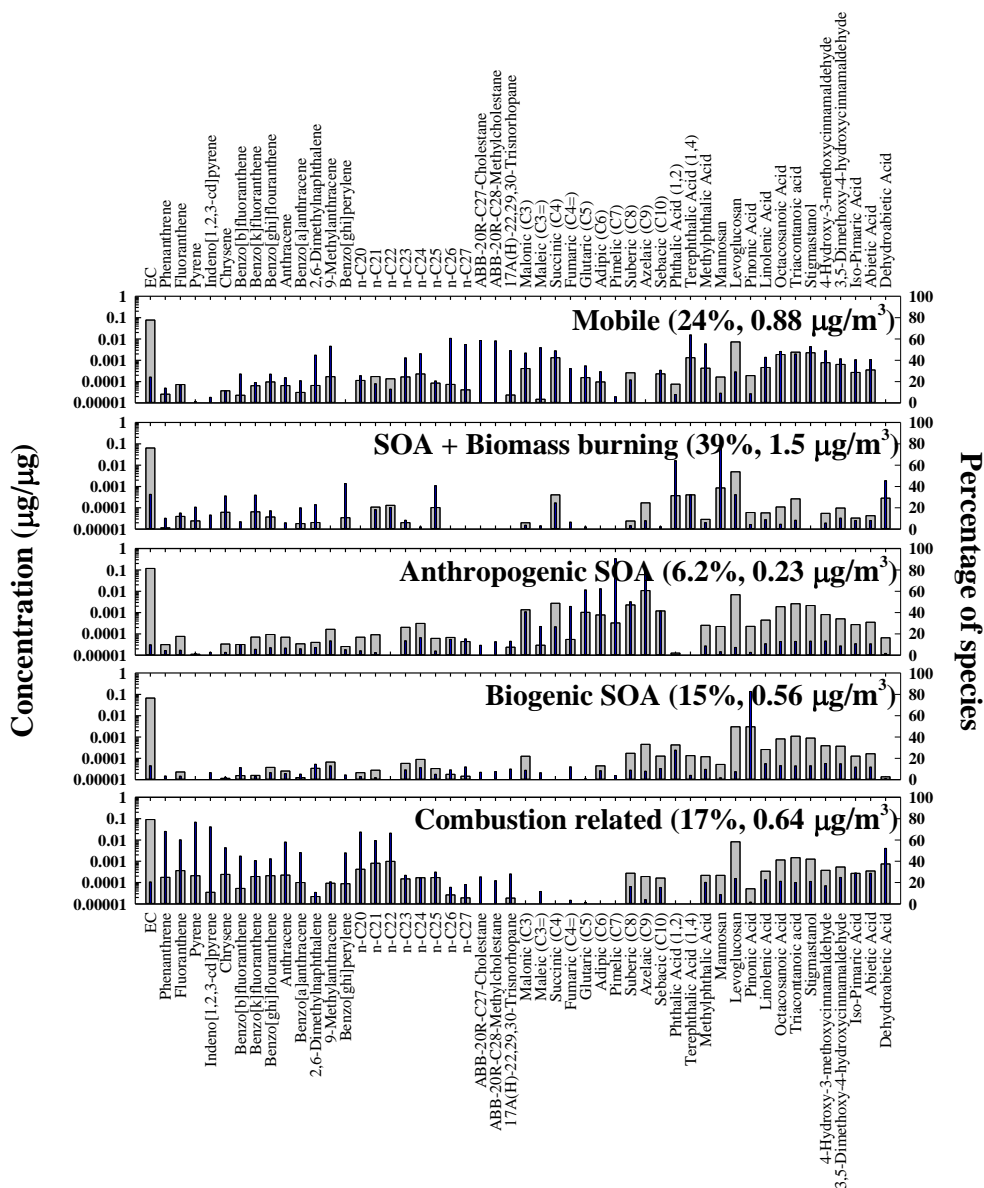


Figure 3. Source profiles of PM₁ OC

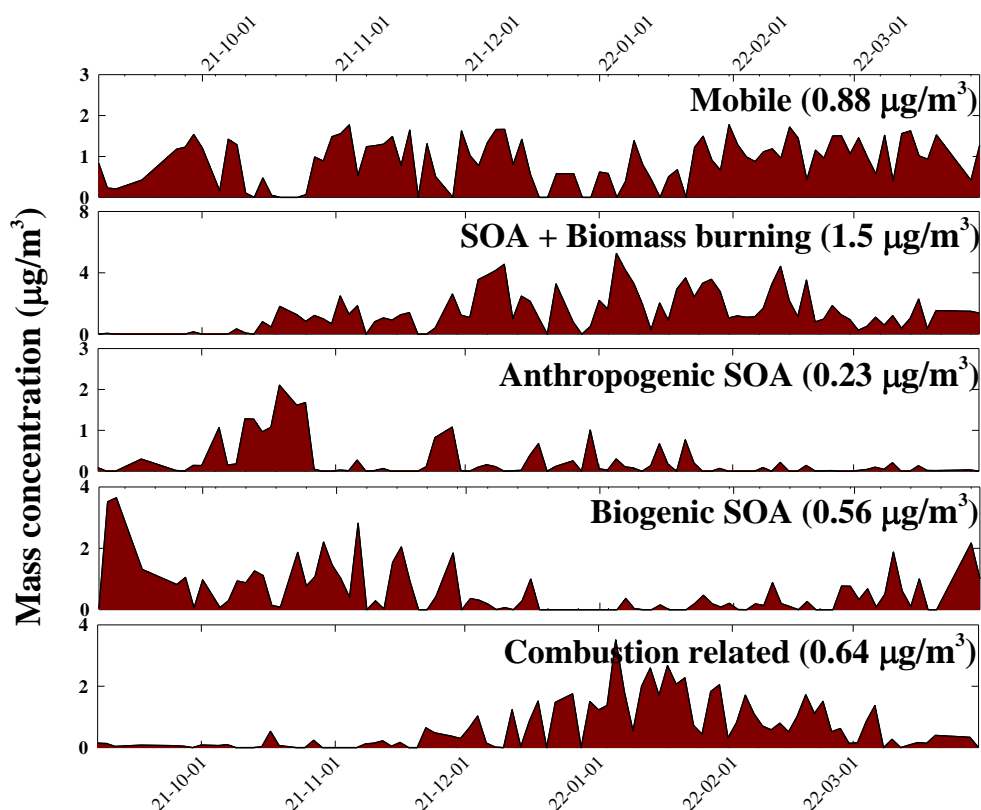


Figure 4. Time series of source contribution

3.2.2. Cluster analysis results

The cluster analysis was performed using 96hr backward trajectory to investigate the air mass flow direction, and 4 clusters were classified as [Figure 5]. The four clusters accounted for as follows: C1 (29%), C2 (30%), C3 (31%), C4 (9%). The cluster 1 was originating from north China, and average contribution of SOA + Biomass burning source was highest at $1.6 \mu\text{g}/\text{m}^3$, and fraction was 41%. The cluster 2 was originating from east China and north Korea, and also average contribution of SOA + Biomass burning source was highest at $1.3 \mu\text{g}/\text{m}^3$, and fraction was 36%. Compared with other clusters, the contribution of biogenic SOA source accounted for the highest fraction (26%) in cluster 2. The cluster 3 and 4 were

originating from Russia and Mongolia, and average contribution of SOA + Biomass burning source was $1.4 \mu\text{g}/\text{m}^3$ and $1.5 \mu\text{g}/\text{m}^3$, respectively. Compared with other clusters, the contribution of combustion related source was increased to 24% and 29%, respectively.

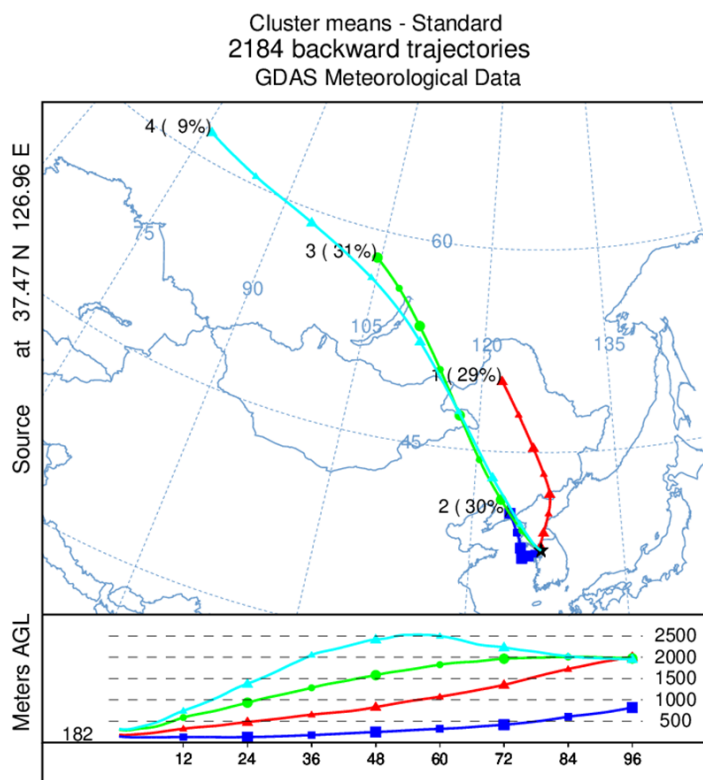


Figure 5. The result of the cluster analysis

Table 6. Average source contribution of each cluster

$\mu\text{g}/\text{m}^3$ (%)	Mobile	SOA + Biomass burning	Anthropogenic SOA	Biogenic SOA	Combustion related
C 1 (29%)	0.97 (25%)	1.6 (41%)	0.26 (7%)	0.56 (14%)	0.53 (13%)
C 2 (30%)	1.0 (28%)	1.3 (36%)	0.16 (4%)	0.99 (26%)	0.24 (6%)
C 3 (31%)	0.72 (20%)	1.4 (37%)	0.30 (8%)	0.39 (11%)	0.87 (24%)
C 4 (9%)	0.81 (22%)	1.5 (42%)	0.2 (3%)	0.13 (4%)	1.1 (29%)

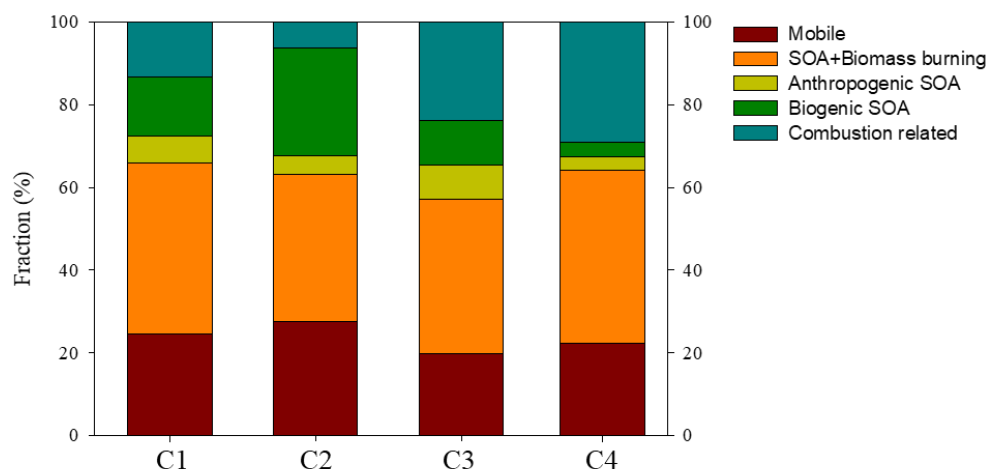


Figure 6. The fraction (%) of source contribution for each cluster

3.2.3. CBPF results

A CBPF model was performed to analyze the source inflow direction at a local scale. The concentration of organic carbon was increased when the wind speed is 2 m/s from the west and northeast directions of the Seoul measurement site. The contribution of mobile source increased when the wind speed is less than 4 m/s from the southwest direction, and this result reflects the location of Gwanak-ro, Yeongdong Expressway, and downtown roads with high traffic

congestion. The contribution of anthropogenic and biogenic sources increased when the wind speed is 4 m/s from the north and east directions, respectively. The contribution of combustion related source increased when the wind speed is 4 m/s from the west direction, while the contribution of SOA + biomass burning source increased when the wind speed less than 4m/s from the west and northeast directions.

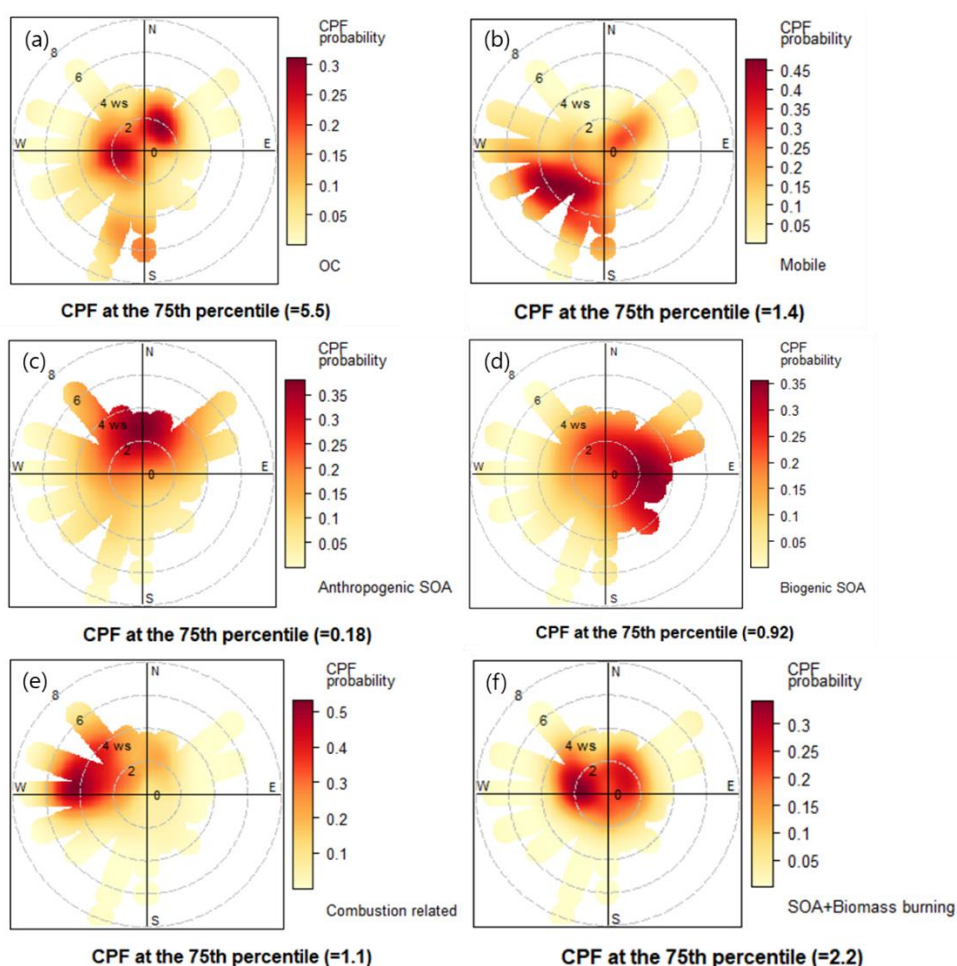


Figure 7. The CBPF results for (a) OC, (b) Mobile, (c) Anthropogenic SOA, (d) Biogenic SOA, (e) Combustion related, (f) SOA + Biomass burning

3.2.4. PSCF results

The PSCF model was performed to identify the potential source areas for long-range transport aerosols using source contributions and 96hr back trajectories. The results for SOA + Biomass burning, Combustion related, Anthropogenic SOA, and Biogenic SOA sources were shown in [Figure 8]. The upper 25% values for each sources were $2.2 \mu\text{g}/\text{m}^3$, $1.1 \mu\text{g}/\text{m}^3$, $0.18 \mu\text{g}/\text{m}^3$, $0.90 \mu\text{g}/\text{m}^3$, respectively. The SOA + Biomass burning source in [Figure 8(a)], Jingjinji(Beijing–Tianjin–Hebei) region, Liaoning province, Mongolia, North Korea were identified as potential source areas. Jingjinji regions are industrial areas with high coal consumption and high emission of air pollutants (Yao et al., 2016). Several studies reported that North Korea regions show high probability as biomass fuel burning source areas influencing the air quality in South Korea (Lee and Kim, 2007, Kim et al., 2013, Kim et al., 2016). Biomass is the major energy source for residential and transportation not only urban areas but also rural areas in North Korea (Von Hippel et al., 2001, Von Hippel et al., 2002, Ashford et al., 2012). The combustion related source in [Figure 8(b)], Mongolia, Inner Mongolia were identified as potential source areas. In Mongolia, coal combustion sources dominate during winter due to the use of coal for heating and power generation (Davy et al., 2011). The anthropogenic SOA source in [Figure 8(c)], Jingjinji regions, Shandong province, Liaoning province, North Korea, Jilin province, Ulaanbaatar were identified as potential source areas. Shandong province is known as a representative anthropogenic emission area (Liu et al., 2017). The biogenic SOA source in [Figure 8(c)], Jingjinji region, Zhengzhou, Jiangsu province, Changdao, Liaoning province, the Yellow sea, and the East sea were identified as potential source areas. Zhengzhou,

the capital of Henan Province, is known for severe air pollution due to the development of coal-based industries (Geng et al., 2013).

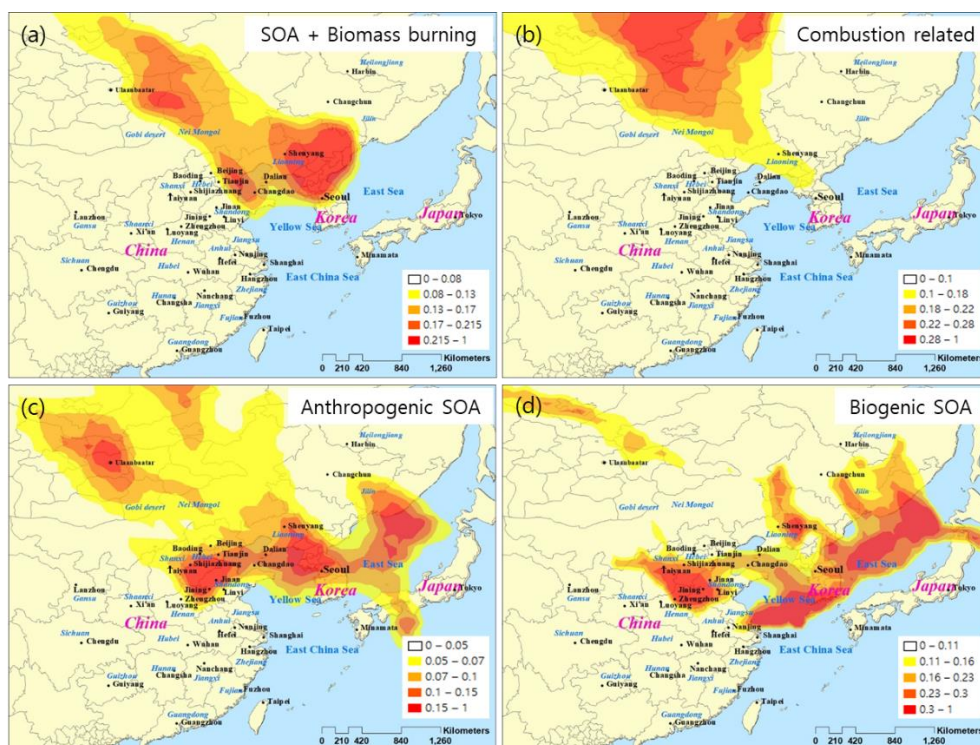


Figure 8. The PSCF results for (a) SOA+Biomass burning, (b) Combustion related, (c) Anthropogenic SOA, (d) Biogenic SOA

3.3. DTT activity results

The oxidative potential value by DTT assay (OP_{dt}) ranged from a minimum of $0.01 \text{ nmol/min/m}^3$ to a maximum of $0.74 \text{ nmol/min/m}^3$, and the average of OP_{dt} was $0.40 \pm 0.18 \text{ nmol/min/m}^3$. The coefficient of determination (R) correlated with OP_{dt} and PM_{10} mass concentration was 0.488, while R correlated with OP_{dt} and PM_{10} OC concentration was 0.740. This result showed that OC has a greater correlation with oxidative potential than mass concentration. To examine the relationship between the oxidative potential of PM_{10} with its source contributions, multiple linear regression analysis was performed [Table 7]. The relative source contribution to the

oxidative potential of PM₁ was estimated according to the derived R² value and the standardized regression coefficients (Beta). Among the sources that contribute to the OP, SOA + Biomass burning and combustion related sources were indicated in this study. Standardized coefficients beta of each source is 0.420, 0.294, respectively. This result indicates that SOA + Biomass burning source was major contributor to OP. Biomass burning which could emit high concentrations of PM with PAHs and volatile organic compounds (VOCs) played a primary role to generate ROS of PM (Simonetti et al., 2018, Weinstein et al., 2017). In addition, the results of statistical analysis of chemical species and DTT consumption rates, pearson correlation coefficient (R) of PAHs is 0.677 ($p < 0.001$), Sugar & Glycerides is 0.654 ($p < 0.001$), Methoxyphenols is 0.503 ($p < 0.001$), Resin acids is 0.563 ($p < 0.001$). These chemical constituents are released from biomass burning, coal and wood combustion (Zhang et al., 2008a).

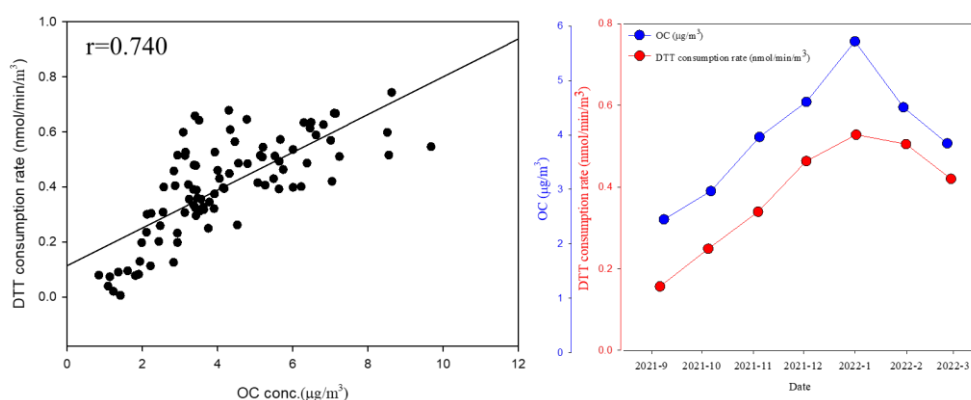


Figure 9. Scatter plot and temporal variation of DTT consumption rate (nmol/min/m³) with OC concentration (µg/m³)

Table 7. Multiple linear regression (MLR) analysis between OP_{dt} and source contributions

	Unstandardized Coefficients (\pm std. error)		Standardized Coefficients (Beta)	R ²
(Constant)	0.387	0.046	–	0.501
SOA+ Biomass burning	0.058	0.012	0.420	
Combustion related	0.067	0.022	0.294	

Table 8. Pearson correlations between the OP_{dt} and the chemical species ($p < 0.001$ level, * $p < 0.01$ level, $p < 0.05$, $p < 0.10$ level)**

	OP _{dt}
PAHs	0.677***
n-Alkanes	0.138
Hopanes & Steranes	0.176*
Aliphatic diacids	0.003
Benzenecarboxylic acids	0.358***
Alkanoic acids	0.352***
Sugar & Glyserides	0.654***
Fatty acids	0.259*
Streols	0.456***
Methoxyphenol	0.503***
Resin acids	0.563***

4. Conclusions

A total of 91 PM₁ samples were collected over seven months (September 2021 to March 2022) at Seoul, Korea. These samples were analyzed for PM₁ mass concentration, organic carbon (OC), elemental carbon (EC), and 56 organic compounds. The average concentrations for entire sampling period of PAHs was 2.8 ± 2.0 ng/m³, n-Alkanes was 13 ± 24 ng/m³, Hopanes & Steranes was 0.03 ± 0.04 ng/m³, Aliphatic diacids was 9.5 ± 8.5 ng/m³,

Benzenecarboxylic acids was $4.0 \pm 2.2 \text{ ng/m}^3$, Alkanoic acids was $7.2 \pm 8.5 \text{ ng/m}^3$, Sugar & Glyserides was $28 \pm 9.5 \text{ ng/m}^3$, Fatty acids was $11 \pm 3.2 \text{ ng/m}^3$, Sterols was $3.9 \pm 0.06 \text{ ng/m}^3$, Methoxyphenols was $2.9 \pm 0.40 \text{ ng/m}^3$, Resin acids was $2.6 \pm 1.6 \text{ ng/m}^3$.

As a results of the PMF model for identifying source contribution, five source categories were identified: Mobile (24%), SOA + Biomass burning (39%), Anthropogenic SOA (6.2%), Biogenic SOA (15%), and Combustion related (17%).

In addition, the cluster analysis, CBPF, and PSCF models were performed to identify the regional and long range transport impacts of each source. The concentration of OC was increased by inflow from the west and northeast directions. The mobile source inflow was dominant from the southwest, and this result reflects the location of Gwanak-ro, Yeongdong Expressway, and downtown roads with high traffic congestion. As for the anthropogenic SOA source, Mongolia, Northeast China, and North Korea were identified as potential source areas through the PSCF model result, and the direction of inflow through the CBPF model result was dominant in the north. As for the biogenic SOA source, Northeast China, the Yellow sea, and the East sea were identified as potential source areas, and the direction of inflow was dominant in the east. The combustion related source had increased contribution in cluster 3 and 4 introduced from relatively long distances. In the PSCF model results, Russia and Mongolia were also identified, and in the CBPF model results, the inflow direction was dominant in the west. The SOA + Biomass burning source accounted for a relatively similar fraction in four clusters. In the PSCF model results, Northeast China, North Korea, and Mongolia were identified, and in the CBPF model results, the west and northeast directions were dominant.

The oxidative potential value by DTT assay (OP_{dtb}) ranged from a minimum of 0.01 nmol/min/ m^3 to 0.74 nmol/min/ m^3 , and the average was 0.40 ± 0.18 nmol/min/ m^3 . To examine the relationship between the OP_{dtb} of PM_{10} with its source contributions, multiple linear regression analysis was performed. The SOA + Biomass burning and combustion related sources were selected as variables representing OP_{dtb} . The standardized coefficients beta of each source is 0.420, 0.294, respectively. This result indicates that SOA + Biomass burning source was major contributor to OP. Biomass burning which could emit high concentrations of PM with PAHs and volatile organic compounds (VOCs) played a primary role to generate ROS of PM (Simonetti et al., 2018, Weinstein et al., 2017). As described above, it was found that sources influenced from long distance regions such as Mongolia, North China, and North Korea had a high correlation with OP. Also, chemical species such as PAHs, sugar & glycerides, methoxyphenols, and resin acids released dominantly from biomass burning, coal and wood combustion were high correlated with OP. Therefore, SOA + Biomass burning source, which contributes the most to OC in Seoul and has a high correlation with OP, must be managed.

References

- ASHFORD, G., DEWS, G. & SMITH, T. 2012. Democratic People's Republic of Korea Environment and Climate Change Outlook. *Ministry of Land and Environment Protection, Pyongyang*.
- BALTENSPERGER, U., KALBERER, M., DOMMEN, J., PAULSEN, D., ALFARRA, M. R., COE, H., FISSEHA, R., GASCHO, A., GYSEL, M. & NYEKI, S. 2005. Secondary organic aerosols from anthropogenic and biogenic precursors. *Faraday Discussions*, 130, 265–278.
- BISWAS, S., VERMA, V., SCHAUER, J. J., CASSEE, F. R., CHO, A. K. & SIOUTAS, C. 2009. Oxidative potential of semi-volatile and non volatile particulate matter (PM) from heavy-duty vehicles retrofitted with emission control technologies. *Environmental Science & Technology*, 43, 3905–3912.
- BRETON, C. V., SALAM, M. T., WANG, X., BYUN, H.-M., SIEGMUND, K. D. & GILLILAND, F. D. 2012. Particulate matter, DNA methylation in nitric oxide synthase, and childhood respiratory disease. *Environmental health perspectives*, 120, 1320–1326.
- CAI, M., ZHANG, S., LIN, X., QIAN, Z., MCMILLIN, S. E., YANG, Y., ZHANG, Z., PAN, J. & LIN, H. 2022. Association of Ambient Particulate Matter Pollution of Different Sizes With In-Hospital Case Fatality Among Stroke Patients in China. *Neurology*.
- CHARRIER, J. G. & ANASTASIO, C. 2012. On dithiothreitol (DTT) as a measure of oxidative potential for ambient particles: evidence for the importance of soluble transition metals. *Atmospheric chemistry and physics (Print)*, 12, 11317.
- CHENG, Y., ZOU, S., LEE, S., CHOW, J., HO, K., WATSON, J., HAN, Y., ZHANG, R., ZHANG, F. & YAU, P. 2011. Characteristics and source apportionment of PM₁ emissions at a roadside station. *Journal of hazardous materials*, 195, 82–91.
- CHO, A. K., SIOUTAS, C., MIGUEL, A. H., KUMAGAI, Y., SCHMITZ, D. A., SINGH, M., EIGUREN-FERNANDEZ, A. & FROINES, J. R. 2005. Redox activity of airborne particulate matter at different sites in the Los Angeles Basin. *Environmental research*, 99, 40–47.
- CHOI, J.-K., HEO, J.-B., BAN, S.-J., YI, S.-M. & ZOH, K.-D. 2012. Chemical characteristics of PM_{2.5} aerosol in Incheon, Korea. *Atmospheric environment*, 60, 583–592.
- DAVY, P. K., GUNCHIN, G., MARKWITZ, A., TROMPETTER, W. J., BARRY, B. J., SHAGJJAMBA, D. & LODOYSAMBA, S. 2011. Air particulate matter pollution in Ulaanbaatar, Mongolia: determination of composition, source contributions and source locations. *Atmospheric Pollution Research*, 2, 126–137.
- FANG, T., VERMA, V., GUO, H., KING, L., EDGERTON, E. & WEBER, R. 2015. A semi-automated system for quantifying the oxidative potential of ambient particles in aqueous extracts using the dithiothreitol (DTT) assay: results from the Southeastern Center for Air Pollution and

- Epidemiology (SCAPE). *Atmospheric Measurement Techniques*, 8, 471–482.
- GAO, B., YU, J.-Z., LI, S.-X., DING, X., HE, Q.-F. & WANG, X.-M. 2011. Roadside and rooftop measurements of polycyclic aromatic hydrocarbons in PM_{2.5} in urban Guangzhou: evaluation of vehicular and regional combustion source contributions. *Atmospheric Environment*, 45, 7184–7191.
- GENG, N., WANG, J., XU, Y., ZHANG, W., CHEN, C. & ZHANG, R. 2013. PM_{2.5} in an industrial district of Zhengzhou, China: Chemical composition and source apportionment. *Particuology*, 11, 99–109.
- HAN, B., DING, X., BAI, Z., KONG, S. & GUO, G. 2011. Source analysis of particulate matter associated polycyclic aromatic hydrocarbons (PAHs) in an industrial city in northeastern China. *Journal of Environmental Monitoring*, 13, 2597–2604.
- HE, L.-Y., HU, M., ZHANG, Y.-H., HUANG, X.-F. & YAO, T.-T. 2008. Fine particle emissions from on-road vehicles in the Zhujiang Tunnel, China. *Environmental science & technology*, 42, 4461–4466.
- HEO, J., DULGER, M., OLSON, M. R., MCGINNIS, J. E., SHELTON, B. R., MATSUNAGA, A., SIOUTAS, C. & SCHAUER, J. J. 2013. Source apportionments of PM_{2.5} organic carbon using molecular marker Positive Matrix Factorization and comparison of results from different receptor models. *Atmospheric Environment*, 73, 51–61.
- HONG, H., YIN, H., WANG, X. & YE, C. 2007. Seasonal variation of PM₁₀-bound PAHs in the atmosphere of Xiamen, China. *Atmospheric Research*, 85, 429–441.
- HOPKE, P. K. 1991. *Receptor modeling for air quality management*, Elsevier.
- JIANG, H., AHMED, C., CANCHOLA, A., CHEN, J. Y. & LIN, Y.-H. 2019. Use of dithiothreitol assay to evaluate the oxidative potential of atmospheric aerosols. *Atmosphere*, 10, 571.
- KIM, I. S., LEE, J. Y. & KIM, Y. P. 2013. Impact of polycyclic aromatic hydrocarbon (PAH) emissions from North Korea to the air quality in the Seoul Metropolitan Area, South Korea. *Atmospheric Environment*, 70, 159–165.
- KIM, I. S., WEE, D., KIM, Y. P. & LEE, J. Y. 2016. Development and application of three-dimensional potential source contribution function (3D-PSCF). *Environmental Science and Pollution Research*, 23, 16946–16954.
- KONG, S., DING, X., BAI, Z., HAN, B., CHEN, L., SHI, J. & LI, Z. 2010. A seasonal study of polycyclic aromatic hydrocarbons in PM_{2.5} and PM_{2.5-10} in five typical cities of Liaoning Province, China. *Journal of Hazardous Materials*, 183, 70–80.
- LEE, J. & KIM, Y. 2007. Source apportionment of the particulate PAHs at Seoul, Korea: impact of long range transport to a megacity. *Atmospheric Chemistry and Physics*, 7, 3587–3596.
- LIN, H., TAO, J., DU, Y., LIU, T., QIAN, Z., TIAN, L., DI, Q., RUTHERFORD, S., GUO, L. & ZENG, W. 2016. Particle size and chemical constituents of ambient particulate pollution associated with cardiovascular mortality in Guangzhou, China. *Environmental Pollution*, 208, 758–766.

- LIN, M. & YU, J. Z. 2019. Dithiothreitol (DTT) concentration effect and its implications on the applicability of DTT assay to evaluate the oxidative potential of atmospheric aerosol samples. *Environmental Pollution*, 251, 938–944.
- LIU, B., WU, J., ZHANG, J., WANG, L., YANG, J., LIANG, D., DAI, Q., BI, X., FENG, Y. & ZHANG, Y. 2017. Characterization and source apportionment of PM_{2.5} based on error estimation from EPA PMF 5.0 model at a medium city in China. *Environmental Pollution*, 222, 10–22.
- LIU, L., BREITNER, S., SCHNEIDER, A., CYRYS, J., BRÜSKE, I., FRANCK, U., SCHLINK, U., LEITTE, A. M., HERBARTH, O. & WIEDENSOHLER, A. 2013. Size-fractionated particulate air pollution and cardiovascular emergency room visits in Beijing, China. *Environmental research*, 121, 52–63.
- LIU, W., XU, Y., LIU, W., LIU, Q., YU, S., LIU, Y., WANG, X. & TAO, S. 2018. Oxidative potential of ambient PM_{2.5} in the coastal cities of the Bohai Sea, northern China: Seasonal variation and source apportionment. *Environmental Pollution*, 236, 514–528.
- MEI, L., YAN, S., LI, Y., JIN, X., SUN, X., WU, Y., LIANG, Y., WEI, Q., YI, W. & PAN, R. 2022. Association between short-term PM₁ exposure and cardiorespiratory diseases: Evidence from a systematic review and meta-analysis. *Atmospheric Pollution Research*, 13, 101254.
- NI, L., CHUANG, C.-C. & ZUO, L. 2015. Fine particulate matter in acute exacerbation of COPD. *Frontiers in physiology*, 6, 294.
- PAATERO, P. 1997. Least squares formulation of robust non-negative factor analysis. *Chemometrics and intelligent laboratory systems*, 37, 23–35.
- POLISSAR, A. V., HOPKE, P. K., PAATERO, P., MALM, W. C. & SISLER, J. F. 1998. Atmospheric aerosol over Alaska: 2. Elemental composition and sources. *Journal of Geophysical Research: Atmospheres*, 103, 19045–19057.
- POPE III, C. A., BURNETT, R. T., TURNER, M. C., COHEN, A., KREWSKI, D., JERRETT, M., GAPSTUR, S. M. & THUN, M. J. 2011. Lung cancer and cardiovascular disease mortality associated with ambient air pollution and cigarette smoke: shape of the exposure-response relationships. *Environmental health perspectives*, 119, 1616–1621.
- RUSSELL, M. & ALLEN, D. T. 2004. Seasonal and spatial trends in primary and secondary organic carbon concentrations in southeast Texas. *Atmospheric Environment*, 38, 3225–3239.
- SCHAUER, J. J., KLEEMAN, M. J., CASS, G. R. & SIMONEIT, B. R. 1999. Measurement of emissions from air pollution sources. 2. C₁ through C₃₀ organic compounds from medium duty diesel trucks. *Environmental science & technology*, 33, 1578–1587.
- SCHAUER, J. J., KLEEMAN, M. J., CASS, G. R. & SIMONEIT, B. R. 2002. Measurement of emissions from air pollution sources. 5. C₁– C₃₂ organic compounds from gasoline-powered motor vehicles. *Environmental science & technology*, 36, 1169–1180.
- SHEESLEY, R. J., SCHAUER, J. J., CHOWDHURY, Z., CASS, G. R. & SIMONEIT, B. R. 2003. Characterization of organic aerosols emitted from the combustion of biomass indigenous to South Asia. *Journal of*

- Geophysical Research: Atmospheres*, 108.
- SHEESLEY, R. J., SCHAUER, J. J., HEMMING, J. D., BARMAN, M. A., GEIS, S. W. & TORTORELLI, J. J. 2004. Toxicity of ambient atmospheric particulate matter from the Lake Michigan (USA) airshed to aquatic organisms. *Environmental Toxicology and Chemistry: An International Journal*, 23, 133–140.
- SHRIVASTAVA, M. K., SUBRAMANIAN, R., ROGGE, W. F. & ROBINSON, A. L. 2007. Sources of organic aerosol: Positive matrix factorization of molecular marker data and comparison of results from different source apportionment models. *Atmospheric Environment*, 41, 9353–9369.
- SIMONETTI, G., CONTE, E., PERRINO, C. & CANEPARI, S. 2018. Oxidative potential of size-segregated PM in an urban and an industrial area of Italy. *Atmospheric Environment*, 187, 292–300.
- TSAPAKIS, M. & STEPHANOU, E. G. 2005. Occurrence of gaseous and particulate polycyclic aromatic hydrocarbons in the urban atmosphere: study of sources and ambient temperature effect on the gas/particle concentration and distribution. *Environmental Pollution*, 133, 147–156.
- VASILAKOS, C., LEVI, N., MAGGOS, T., HATZIANESTIS, J., MICHPOULOS, J. & HELMIS, C. 2007. Gas-particle concentration and characterization of sources of PAHs in the atmosphere of a suburban area in Athens, Greece. *Journal of hazardous materials*, 140, 45–51.
- VERMA, V., FANG, T., GUO, H., KING, L., BATES, J., PELTIER, R., EDGERTON, E., RUSSELL, A. & WEBER, R. 2014. Reactive oxygen species associated with water-soluble PM 2.5 in the southeastern United States: spatiotemporal trends and source apportionment. *Atmospheric Chemistry and Physics*, 14, 12915–12930.
- VON HIPPEL, D., SAVAGE, T. & HAYES, P. 2002. The DPRK energy sector: estimated year 2000 energy balance and suggested approaches to sectoral redevelopment. *hereafter “Sectoral Redevelopment”*, Report Prepared for the Korea Energy Economics Institute, Nautilus Institute (revised March 6, 2003), 2.
- VON HIPPEL, D. F., HAYES, P., WILLIAMS, J. H., GREACEN, C., SAGRILLO, M. & SAVAGE, T. 2001. RURAL ENERGY SURVEY IN UNHARI VILLAGE, THE DEMOCRATIC PEOPLE’S REPUBLIC OF KOREA (DPRK): METHODS, RESULTS, AND. *Nautilus*.
- WEINSTEIN, J. R., ASTERIA-PEÁALOZA, R., DIAZ-ARTIGA, A., DAVILA, G., HAMMOND, S. K., RYDE, I. T., MEYER, J. N., BENOWITZ, N. & THOMPSON, L. M. 2017. Exposure to polycyclic aromatic hydrocarbons and volatile organic compounds among recently pregnant rural Guatemalan women cooking and heating with solid fuels. *International journal of hygiene and environmental health*, 220, 726–735.
- WU, X., VU, T. V., SHI, Z., HARRISON, R. M., LIU, D. & CEN, K. 2018. Characterization and source apportionment of carbonaceous PM_{2.5} particles in China–A review. *Atmospheric Environment*, 189, 187–212.
- XINGRU, L., XUEQING, G., XINRAN, L., CHENSHU, L., ZHANG, S. & YUESI, W. 2009. Distribution and sources of solvent extractable organic

- compounds in PM_{2.5} during 2007 Chinese Spring Festival in Beijing. *Journal of Environmental Sciences*, 21, 142–149.
- YANG, A., JEDYNSKA, A., HELLACK, B., KOOTER, I., HOEK, G., BRUNEKREEF, B., KUHLBUSCH, T. A., CASSEE, F. R. & JANSSEN, N. A. 2014. Measurement of the oxidative potential of PM_{2.5} and its constituents: The effect of extraction solvent and filter type. *Atmospheric Environment*, 83, 35–42.
- YAO, L., YANG, L., YUAN, Q., YAN, C., DONG, C., MENG, C., SUI, X., YANG, F., LU, Y. & WANG, W. 2016. Sources apportionment of PM_{2.5} in a background site in the North China Plain. *Science of the Total Environment*, 541, 590–598.
- ZHANG, T., CLAEYS, M., CACHIER, H., DONG, S., WANG, W., MAENHAUT, W. & LIU, X. 2008a. Identification and estimation of the biomass burning contribution to Beijing aerosol using levoglucosan as a molecular marker. *Atmospheric Environment*, 42, 7013–7021.
- ZHANG, Y., SCHAUER, J. J., ZHANG, Y., ZENG, L., WEI, Y., LIU, Y. & SHAO, M. 2008b. Characteristics of particulate carbon emissions from real-world Chinese coal combustion. *Environmental science & technology*, 42, 5068–5073.
- ZHANG, Y. Y., MÜLLER, L., WINTERHALTER, R., MOORTGAT, G. K., HOFFMANN, T. & PÖSCHL, U. 2010. Seasonal cycle and temperature dependence of pinene oxidation products, dicarboxylic acids and nitrophenols in fine and coarse air particulate matter. *Atmos. Chem. Phys.*, 10, 7859–7873.

Supplementary Materials

Table S 1. Operating conditions of OC/EC analyzer

Step	Carrier Gas	Ramp Time (sec)	Program Temperature (°C)
1	Helium	60	315
2	Helium	60	475
3	Helium	60	615
4	Helium	90	870
	Helium	Oven heaters are turned off to cool down	
5	2% Ox in He	45	550
6	2% Ox in He	45	625
7	2% Ox in He	45	700
8	2% Ox in He	45	775
9	2% Ox in He	45	850
10	2% Ox in He	120	910
	Cal Gas + Helium/Ox	External Std. Calibration and cool-down	

Table S 2. Operating conditions of GC/MS

Category	Analysis condition
	DB-5MS
GC column	(30m, 0.25 μ m film thickness, 0.25mm i.d.)
Carrier gas	Ultra high purity He (99.9%)
Injection vol.	1 μ l
Injection mode	Splitless mode
Injection temp.	280°C
Analysis temp.	maintain at 60°C for 1 min, Raise the temp. to 310°C at a speed of 4°C/min, maintain at 310°C for 15 min.
Ionization energy	70 eV (EI mode)
Mass range	40~600 Da
Quadrupole temp.	150°C
Ion source temp.	230°C
Transfer line temp.	280°C

Table S 3. GC/MS MDLs

Compounds	MDLs (ng/m ³)	Compounds	MDLs (ng/m ³)
PAHs		n-Alkanes	
2,6-Dimethylnaphthalene	0.061	n-C20	0.355
Phenanthrene	0.041	n-C21	0.185
Anthracene	0.051	n-C22	0.290
9-Methylanthracene	0.062	n-C23	0.338
Fluoranthene	0.056	n-C24	0.512
Pyrene	0.022	n-C25	0.173
Benzo [ghi] fluoranthene	0.013	n-C26	0.172
Benzo [a] anthracene	0.022	n-C27	0.125
Chrysene	0.033		
Benzo [b] fluoranthene	0.125	Hopanes & Steranes	
Benzo [k] fluoranthene	0.120	ABB-20R-C27- Cholestane	0.001
Indeno [1,2,3-cd] pyrene	0.029	ABB-20R-C28- Methylcholestane	0.005
Benzo [ghi] perylene	0.067	17A (H) - 22,29,30- Trisnorhopane	0.070

Table S 4. GC/MS MDLs (Continued)

Compounds	MDLs (ng/m ³)	Compounds	MDLs (ng/m ³)
Aliphatic diacids		Sugar & Glyserides	
Malonic (C3)	0.338	Mannosan	0.063
Maleic (C3=)	0.036	Levogluconan	1.013
Succinic (C4)	0.164	Monopalmitin (16:0)	0.113
Fumaric (C4=)	0.042	Monostearin (18:0)	0.053
Glutaric (C5)	0.071	Fatty acids	
Adipic (C6)	0.323	Pinonic acid	0.164
Pimelic (C7)	0.041	Linoleic acid	0.186
Suberic (C8)	0.119	Octacosanoic acid	1.488
Azelaic (C9)	0.160	Tricontanoic acid	1.966
Sebacic (C10)	0.097		
Benzenecarboxylic acids		Sterol	
Phthalic acid (1,2)	0.343	Stigmastanol	0.152
Terephthalic acid (1,4)	0.192	Methoxyphenols	
Methylphthalic acids	0.135	4-Hydroxy-3-methoxycinnamaldehyde	0.109
Alkanoic acids		3,5-Dimethoxy-4-hydroxycinnamaldehyde	0.100
C16:0	2.970	Resin acids	
C18:0	2.118	Iso-Pimaric acid	0.077
C20:0	1.033	Abietic acid	0.100
C22:0	0.413	Dehydroabietic acid	0.053
C24:0	0.420		

국문 초록

서울시 PM₁ 유기화학적 성분의 오염원 추정과 산화 잠재력 평가

류지원

환경보건학과

서울대학교 보건대학원

대한민국 서울은 상업, 산업, 그리고 주거 지역이 발달한 도시로서 다양한 지역적 오염원이 존재하고, 또한 주변 국가들로부터 장거리 이동하는 오염원의 영향 또한 받기 때문에 매우 복잡한 대기 조성을 가진다. 특히 도시나 산업지역에서는 유기탄소와 원소탄소의 구성비가 높다. 따라서 서울시 대기 중 유기성분의 화학적 특성과 오염원을 파악하고 그의 건강영향을 평가하는 연구는 적절한 대기오염 저감 정책 수립을 위해서 필수적으로 이루어져야 한다. 이 연구는 서울시 유기성분의 오염원과 그 기여도를 e정량적으로 파악했고, 산화잠재력을 평가하여 건강영향을 추정하였다.

2021년 9월부터 2022년 3월까지 대한민국 서울 관측지점에서 포집된 91개의 PM₁ 시료에 대하여 질량 농도, Organic Carbon (OC), Elemental Carbon (EC), 56종의 유기화학적 성분에 대한 분석을 수행하였다. 화학분석결과를 바탕으로, 오염원 기여도 추정 연구를 위해 Positive Matrix Factorization (PMF) 모델을 수행했다. 그 결과, 자동차 (24%), 이차생성유기 에어로졸 + 생물성 연소 (39%), 인위적 이차생성유기 에어로졸 (6.2%), 생물성 이차생성유기 에어로졸 (15%), 그리고 소각 관련 오염원 (17%) 5개의 오염원으로 분리되었다. 이에 더하여, 장거리 이동 오염원의 고농도 발생 가능 지역을 추정하기 위해

Potential Source Contribution Function (PSCF)을 수행했고, 지역적 오염원의 유입 방향을 추정하기 위해 Conditional Bivariate Probability Function (CBPF) 모델을 수행했다.

산화 잠재력 평가를 위한 Dithiothreitol (DTT) assay 결과, 몽골, 중국 북부지역, 북한 등 장거리 지역에서 유입되는 영향을 받는 이차생성유기 에어로졸 + 생물성 연소 오염원이 산화잠재력에 가장 크게 기여하는 것으로 나타났다. 또한, 생물성 연소, 나무, 석탄 소각에서 주로 배출된다고 알려진 PAHs, sugars, glycerides, methoxyphenols, resin acids 성분이 산화잠재력과 상관성을 가지는 것으로 나타났다. 그러므로, 서울시 대기 중 유기성분에 가장 크게 기여하고 산화잠재력과 상관성이 큰 이차생성유기 에어로졸 + 생물성 연소 오염원은 반드시 관리되어야 한다고 판단된다.

주요 단어: PM₁, 유기성분, 오염원 추정, 산화잠재력

학번: 2020-20616